NASA TECHNICAL NOTE

NASA TN D-3709

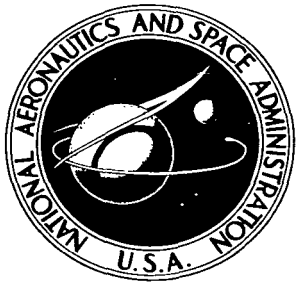

NASA TN D-3709

MEASUREMENT OF EFFECTIVE DELAYED NEUTRON FRACTION FOR NASA ZERO POWER REACTOR I

by Donald Alger, Wendell Mayo, and Robert Mueller

Lewis Research Center

Cleveland, Ohio

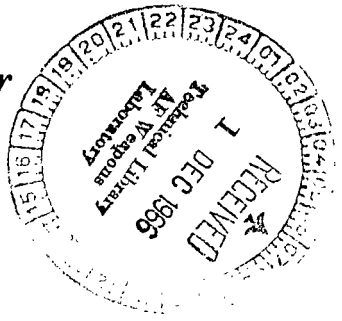

NATIONAL AERONAUTICS AND SPACE ADMINISTRATION • WASHINGTON, D. C. • NOVEMBER 1966

NASA TN D-3709

MEASUREMENT OF EFFECTIVE DELAYED NEUTRON FRACTION FOR NASA ZERO POWER REACTOR I

By Donald Alger, Wendell Mayo, and Robert Mueller

Lewis Research Center
Cleveland, Ohio

NATIONAL AERONAUTICS AND SPACE ADMINISTRATION

For sale by the Clearinghouse for Federal Scientific and Technical Information
Springfield, Virginia 22151 – Price $2.00

MEASUREMENT OF EFFECTIVE DELAYED NEUTRON FRACTION FOR NASA ZERO POWER REACTOR I

by Donald Alger, Wendell Mayo, and Robert Mueller

Lewis Research Center

SUMMARY

The effective delayed neutron fraction β_{eff} has been experimentally determined for each of three uranyl fluoride - water solution reactors in the NASA Zero Power Reactor I facility. The hydrogen to uranium 235 atom ratios R for the solutions in these measurements are 190, 473, and 565. The value of β_{eff} has been measured by the boron substitution method. Values for β_{eff} obtained are 0.0090 ± 0.0006, 0.0086 ± 0.0005, and 0.0082 ± 0.0004 for the respective atom ratios. Calculated values of β_{eff} are in reasonable agreement with the experimental results.

INTRODUCTION

The inhour method (ref. 1) is a kinetic technique that is commonly used to measure the reactivity associated with perturbations to a delayed critical reactor. The reactivity is measured in terms of the effective delayed neutron fraction β_{eff}. This effective delayed neutron fraction is usually chosen as the unit of reactivity and called the dollar (ref. 2).

The effective delayed neutron fraction β_{eff} for a given reactor differs from the delayed neutron fraction β (ref. 14) because the delayed neutrons are emitted with a lower average energy (~0.5 MeV) than the prompt neutrons (~2 MeV). Delayed neutrons therefore have a smaller leakage probability, and their effectiveness in causing new fissions in a thermal reactor core is greater than the prompt neutrons. Effects on β_{eff} due to uranium 238 fast fissions do not occur since nearly all of the delayed neutrons are emitted below the uranium 238 fission energy threshold (~0.8 MeV). Therefore, interaction of delayed neutrons with fast fissions in uranium 238 is a very small effect in uranyl fluoride solution reactors that are essentially thermal reactors. Values of β_{eff} or the ratios of

β_{eff} to $\beta(\equiv\gamma)$, are functions of the composition and geometry of the reactors involved (refs. 3 and 4).

The NASA Zero Power Reactor I (ZPR-I) is a uranyl fluoride - water (UO_2F_2-H_2O) system with criticality achieved by varying solution height. A wide range of uranium 235 loadings is possible depending on the solution density. A measure of the loading is the hydrogen to uranium 235 atom ratio R. Criticality in the unreflected system may be achieved with less than 3 kilograms of uranium 235 with R values ranging from approximately 180 to 570.

There were two objectives of this study, one of which was to determine β_{eff} for several uranyl fluoride - water solution concentrations. (A calibration curve relating the primary measurement, or the change in fuel solution height, to absolute reactivity may then be constructed.) The other objective was to test calculational techniques that may be used to extend these results to other reactor configurations.

Gwin and Weinberg (ref. 5) determined β_{eff} for several uranyl fluoride - water solution reactors using experimentally determined bucklings. The measurement of β_{eff} was not the primary objective of that study and the results were approximate. The method required reactors of various solid configurations (spheres, cylinders, etc.). Ruane, et al. (ref. 6), Kaplan and Henry (ref. 7), and Perez-Belles, Kington, and DeSaussure (ref. 8) used the boron substitution technique for the measurement of β_{eff} in their respective reactors. The measurements reported herein for the ZPR-I reactor follow the methods of reference 8. The calculational method employed follows that reported in reference 7. In both cases, some modification and extension of the theory is necessary for application to the ZPR-I reactor.

The following section presents the theory of the experiment. Next follow the experimental procedure, the description of the equipment, and the measurements and results, followed by the theoretical calculations for β_{eff}.

THEORY OF THE EXPERIMENT

The theory of the experiment is based on two expressions for the reactivity due to perturbations to a critical reactor, the inhour equation, and the time-independent perturbation equation. Application of these two equations yields an expression for β_{eff} which, in many reactors, is well suited to experimental evaluation. The results have been applied, for example, to the Bulk Shielding Reactor-I at the Oak Ridge National Laboratory (ref. 8). The notation used in reference 8 is used here when applicable. The ZPR-I measurements for β_{eff} depend on modification and extension of the results given in reference 8. The reasons for this and the problems presented are discussed as the theory is developed.

It is assumed that a nonfissionable material exists whose scattering and absorption cross sections at every energy are identical with those of the fuel. If a small amount of this material is substituted for an equal volume of fuel in a critical reactor, the perturbed reactor will have a reactivity given by the inhour equation

$$\delta\rho_{\tau_i} = \frac{\ell}{T_i} + \frac{\beta_{eff}}{\beta} \sum_{j=1}^{6} \frac{\beta_j}{(1 + \lambda_j T_i)} \tag{1}$$

Symbols are defined in appendix A.

It is assumed that the substitution in a small region of volume τ_i results in a long stable reactor period T_i, which is greater than 200 seconds for these experiments. The mean prompt neutron lifetime ℓ for the ZPR-I varies considerably with fuel solution concentration, but it is of the order of 40 microseconds for the range of concentrations studied. Thus, the term ℓ/T_i in equation (1) may be neglected for these measurements.

The same reactivity for a perturbed reactor is given by the time-independent perturbation equation

$$\delta\rho_{\tau_i} = \frac{\int_{\tau_i} d\underline{r} \int dE\, \delta\nu\Sigma_f(\underline{r}, E)\Phi(\underline{r}, E)P^*(\underline{r})}{\int_V d\underline{r} \int dE\, \nu\Sigma_f(\underline{r}, E)\Phi(\underline{r}, E)P^*(\underline{r}) - \int_{\tau_i} d\underline{r} \int dE\, \nu\Sigma_f(\underline{r}, E)\Phi(\underline{r}, E)P^*(\underline{r})} \tag{2}$$

where the fission spectrum weighted neutron importance is

$$P^*(\underline{r}) = \int dE' f(E')\Phi^*(\underline{r}, E')$$

In principle, only a single substitution is necessary since the measured quantity is the reactor period; hence, if equation (2) can be evaluated with sufficient accuracy, β_{eff} can be found from equations (1) and (2). Equation (2) may be evaluated in several ways, depending on the assumptions made. Henry (ref. 9) has shown that two static multigroup spatial solutions in which the geometry is accurately represented can be used to obtain $\delta\rho_{\tau_i}$ fully in agreement with equation (2). In performing a substitution experiment for the effective delayed neutron fraction in a solid fueled reactor, Kaplan and Henry (ref. 7) chose to sum the results obtained experimentally for successive substitutions in different fueled regions and to sum the results obtained by evaluation of equation (2) using four

energy group spatial flux and adjoint calculated solutions to get the best value for β_{eff}, that is,

$$\sum \left(\delta\rho_{\tau_i}\right)_{calc} = \sum \left(\delta\rho_{\tau_i}\right)_{exp}$$

If equation (1) is used, it follows that

$$\beta_{eff} = \frac{\sum_i \left(\delta\rho_{\tau_i}\right)_{calc}}{\sum_i \left(\sum_{j=1}^{6} \frac{\beta_j/\beta}{1+\lambda_j T_i}\right)_{i,\,exp} \left[\text{sign}\left(\delta\rho_{\tau_i}\right)_{calc}\right]} \tag{3}$$

where i represents the i^{th} substitution and $\left[\text{sign}\left(\delta\rho_{\tau_i}\right)_{calc}\right]$ is negative when $\delta\rho_{\tau_i}$ is negative and positive when $\delta\rho_{\tau_i}$ is positive.

If, however, successive substitutions are made over the entire fueled region of the core, or at least over symmetric regions, equation (3) reduces to an expression involving only experimentally determined periods. To show this, equation (2) is summed over all regions τ_i that make up the total core volume V. A period measurement is made for each substitution and care is taken not to overlap regions. The substitutions must result in a small but well defined reactivity change. Equation (2) is now written as

$$\sum \delta\rho_{\tau_i} = \frac{\int_V d\underline{r} \int dE\, \delta\nu\Sigma_f(\underline{r}, E)\Phi(\underline{r}, E)P^*(\underline{r})}{\int_V d\underline{r} \int dE\, \nu\Sigma_f(\underline{r}, E)\Phi(\underline{r}, E)P^*(\underline{r}) - \left\langle \int_{\tau_i} d\underline{r} \int dE\, \nu\Sigma_f(\underline{r}, E)\Phi(\underline{r}, E)P^*(\underline{r}) \right\rangle} \tag{4}$$

where the second term in the denominator of equation (4) is an average for all substitutions of that quantity. Since, for these experiments, the second term in the denominator of equation (4) is small compared to the first term, it may be neglected. For these experiments, it follows that

$$\delta\nu\Sigma_f = -\nu\Sigma_f$$

and therefore

$$\sum_i \delta\rho_{T_i} = -1 \tag{5}$$

Hence, equation (3) may be written as

$$\beta_{eff} = \frac{-1}{\sum_i \left(-\sum_{j=1}^{6} \frac{\beta_j/\beta}{1 + \lambda_j T_i} \right)_i} \tag{6}$$

A correction to equations (5) and (6) usually must be made to account for the mismatch in cross sections between the fuel and the substitute. If the materials for the substitute are chosen properly, then the only mismatch of any consequence is due to the absorption cross section. The correction may be obtained by using the absorption term from the time-independent perturbation equation as

$$\delta A = \frac{\int_V d\underline{r} \int dE \delta\Sigma_a(\underline{r}, E)\Phi(\underline{r}, E)\Phi^*(\underline{r}, E)}{\int_V d\underline{r} \int dE \nu\Sigma_f(\underline{r}, E)\Phi(\underline{r}, E)P^*(\underline{r})} \tag{7}$$

where the second term in the denominator is omitted. The correction is usually small and, for these experiments, did not exceed 0.2 percent. Equation (6) is now rewritten to include this corrected δA as

$$\beta_{eff} = -\frac{1 - \delta A}{\sum_i \left(-\sum_{j=1}^{6} \frac{\beta_j/\beta}{1 + \lambda_j T_i} \right)_i} \tag{8}$$

Because the ZPR-I utilizes the uranyl fluoride fuel solution, it is impractical to attempt substitutions that map out the entire fuel volume, or even a symmetric segment of the fuel. Use is made of the fact noted in equation (2) that the reactivity is proportional to the product of the power and fission spectrum weighted adjoint; that is,

$$\delta\rho_{\tau_i} \propto \int_{\tau_i} d\underline{r} \int dE\, \nu\Sigma_f(\underline{r}, E)\Phi(\underline{r}, E)P^*(\underline{r}) \equiv \int_{\tau_i} P(\underline{r})P^*(\underline{r})d\underline{r} \tag{9}$$

where

$$P(\underline{r}) = \int dE\, \nu\Sigma_f(\underline{r}, E)\Phi(\underline{r}, E)$$

Several substitutions of small, but different, volumes at the same position in the core allow the experimental specific reactivity ρ_s to be determined, and equation (8) becomes

$$\beta_{eff} = -\frac{1 - \delta A}{\frac{\rho_s}{\beta}\int_V P(\underline{r})P^*(\underline{r})d\underline{r}} \tag{10}$$

where the $P(\underline{r})$ and $P^*(\underline{r})$ are normalized such that

$$-\sum_j \frac{\beta_j/\beta}{1 + \lambda_j T_i} = \frac{\rho_s}{\beta}\int_{\tau_i} P(\underline{r})P^*(\underline{r})d\underline{r} \tag{11}$$

If the extrapolation distances at the boundaries of an unreflected reactor are assumed to be energy independent, then $P(\underline{r})$ and $P^*(\underline{r})$ have the same spatial distribution; $\Phi(\underline{r})$ and $\Phi^*(\underline{r})$ also have the same spatial distributions, where

$$\Phi(\underline{r}) = \int dE\Phi(\underline{r}, E)$$

and

$$\Phi^*(\underline{r}) = \int dE\Phi^*(\underline{r}, E)$$

Equation (10) is rewritten as

$$\beta_{eff} = -\frac{1 - \delta A}{\frac{\rho_s}{\beta}\int \Phi(\underline{r})\Phi^*(\underline{r})d\underline{r}} \tag{12}$$

where the integral in the denominator is normalized as in equation (11). This expression

is used for the determination of β_{eff}. The experimental and computational procedures are described in the following sections.

EXPERIMENTAL PROCEDURE

Reactor Description

The ZPR-I is an unreflected (bare) cylindrical reactor utilizing a uranyl fluoride - water solution as fuel and moderator. It is, therefore, a homogeneous thermal reactor. Criticality, for a given fuel concentration, is achieved by varying the fuel solution height. The height is measured by a micrometer lead screw with a platinum electrical continuity probe attached. The uranium is enriched to 93.2 percent uranium 235. The aluminum tank has a 30.48-centimeter inside diameter with a 0.3175-centimeter-thick wall. The critical height varies between approximately 23 and 76 centimeters depending on the fuel solution concentration.

Direct measurement of the stable reactor period that would result if a neutron absorber were inserted or removed from a ZPR-I core is not possible, since no means are available for the remote movement of an experiment into or out of an already critical ZPR-I core. Therefore, the reactivity associated with a neutron absorber placed into a ZPR-I core must be obtained indirectly by measuring the critical height of an unperturbed core, shutting the reactor down by draining the solution, and then positioning the absorber in the core and measuring the new critical height of the solution. The difference in critical height measurements must then be related to reactivity by a previously obtained calibration curve. A ZPR-I calibration curve, and a discussion of its determination, is presented in appendix B.

The ZPR-I base cores chosen for these experiments had critical heights of 24.892 centimeters (9.800 in.), 45.720 centimeters (18.000 in.), and 67.310 centimeters

TABLE I. - FUEL SOLUTION CONSTANTS OF ZERO POWER REACTOR I BASE CORES

Base core critical height at 20° C, cm	Uranyl fluoride - water solution density at 20° C, gm/cm^3	Uranyl fluoride - water atom concentration, N, atoms/cm^3					Hydrogen to uranium 235 atom ratio, R	Macroscopic neutron absorption cross section, Σ_A(0.0253 eV), cm^{-1} (a)
		Hydrogen	Uranium 235	Uranium 238	Oxygen	Fluorine		
24.892	1.1672	6.5505×10^{22}	3.4463×10^{20}	0.2511×10^{20}	3.3492×10^{22}	7.3947×10^{20}	190.1	0.2609
45.720	1.0671	6.6263	1.4005	.1021	3.3432	3.0052	473.1	.1191
67.310	1.0559	6.6346	1.1726	.08545	3.3424	2.5161	565.8	.1033

[a] σ_A(0.0253 eV) from table II.

TABLE II. - MICROSCOPIC NEUTRON ABSORPTION CROSS SECTIONS

Element	Microscopic neutron absorption cross section, σ_A(0.0253 eV), b
Hydrogen	0.33
Uranium 235	694.0
Uranium 238	2.71
Oxygen	20×10^{-5}
Fluorine	.01
Boron (natural)	762.0

(26.500 in.). Fuel solution constants for these base cores are given in table I (p. 7). The macroscopic neutron absorption cross sections Σ_A(0.0253 eV) are calculated from the atom concentrations of table I, and the microscopic neutron absorption cross sections σ_A(0.0253 eV) in table II.

The critical height of a solution reactor decreases slightly from day to day because of the evaporation of water from the fuel solution. It is not feasible, however, to add water each day to make up for the evaporation loss. As a result, the unperturbed critical solution height during a series of measurements does not remain constant. Evaporation of water from the uranyl fluoride - water fuel solution is, however, essentially a uniform perturbation of the solution Σ_A(0.0253 eV) with a certain reactivity worth relative to some chosen base critical height. Each of the experiments can be corrected to the base core height by use of the calibration curve in appendix B.

Boron-for-Fuel Substitution

Pure analytical reagent grade boric acid crystals dissolved in water were used as a substitute for fuel. The boron content of the boric acid solutions was specified by equating the macroscopic thermal neutron absorption cross section (Σ_A(0.0253 eV)) of a particular uranyl fluoride - water solution, in which the substitution was to be made, to that of the boric acid solution. The boric acid solutions were prepared at Lewis.

Five thin-walled plastic spheres were fabricated. Volumes of the spheres are shown in table III. A 0.1588-centimeter-diameter (1/16-in. -diam) filling hole was tapped in the surface of each ball and sealed with a threaded plastic screw and a neoprene O-ring. Volumes were determined by filling these spheres with 20° C demineralized water, weighing, and then calculating each volume from the mass of water and known absolute density of water at 20° C (0.998203 g/cm^3). In determinining the volumes, care was taken to remove all air bubbles.

TABLE III. - VOLUMES OF SPHERICAL PLASTIC CONTAINERS USED FOR BORON-FOR-FUEL SUBSTITUTION MEASUREMENTS

Plastic ball number	Ball volume, cm^3
1	28.3000
2	19.3249
3	9.4124
4	6.3727
5	4.6477

For the experiments, the spheres were filled with either boric acid solution or fuel

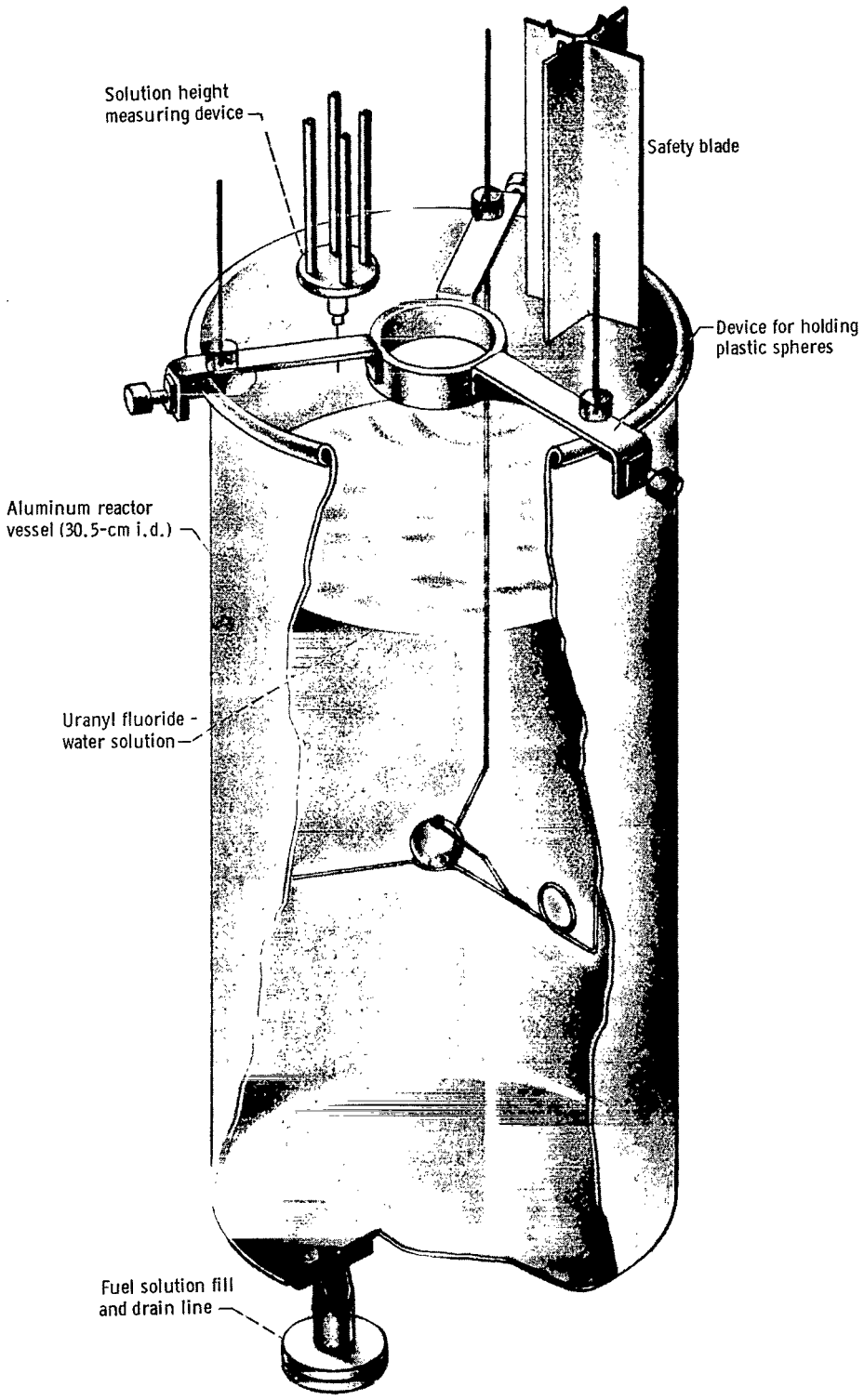

Figure 1. - Schematic of ZPR-I, reactor showing plastic ball centrally positioned in core.

solution and positioned in the core by a stainless-steel wire holder. A sketch of the ZPR-I with a plastic sphere held in the core center is shown in figure 1 (p. 9).

For each base core, three concentrations of boric acid solution were prepared that would bracket the solution $\Sigma_A(0.0253\ eV)$. This is necessary since the $\Sigma_A(0.0253\ eV)$ of the uranyl fluoride - water solution varies slightly with time because of evaporation of water from the solution. Prior to a substitution experiment, a sample of ZPR-I solution was removed and its density measured at 20° C. Uranium 235 and other constituent atom densities N, in atoms per cubic centimeter of solution, were determined from previously obtained experimental data relating fuel solution density at 20° C and uranium atom content as determined by a chemical analysis (ref. 10). Atom densities, microscopic and macroscopic absorption cross sections for the fuel, and boric acid solutions are given in tables I, II, and IV.

Measurement of the boron-for-fuel substitution reactivity worth for each base core involved first filling the five plastic balls (see table III, p. 8) with uranyl fluoride - water solution of the base core. No attempt was made to remove completely all air bubbles from the balls when they were filled with fuel. Consequently, a small air bubble remained. This filled volume was calculated from the mass of fuel in a ball and the measured fuel density. Air bubble volumes equalled the difference between the fuel volume in the ball and the volumes in table III. After the measurement of the reactivity worths

TABLE IV. - DATA FOR BORIC ACID SOLUTION CONCENTRATIONS USED AS BORON-FOR-FUEL SUBSTITUTIONS IN ZERO POWER REACTOR I BASE CORES

Base core solution		Concentration of boric acid solution, g solute/cm^3	Boric acid solution	
Critical height at 20° C, cm	Macroscopic neutron absorption cross section at 0.0253 eV, $\Sigma_A(0.0253\ eV)$, cm^{-1}		Density, gm/cm^3	Macroscopic neutron absorption cross section at 0.0253 eV, $\Sigma_A(0.0253\ eV)$, cm^{-1}
24.892	0.2609	0.028987	1.00888	0.2371
	.2609	.031938	1.00993	.2590
	.2609	.035008	1.01111	.2817
45.720	0.1191	0.011579	1.00246	0.1079
	.1191	.013602	1.00317	.1229
	.1191	.016040	1.00410	.1410
67.310	0.1033	0.01001	1.00189	0.09628
	.1033	.01201	1.00262	.1111
	.1033	.01402	1.00337	.1261

of all five fuel-filled spheres, the fuel was removed. Each sphere was then rinsed several times with demineralized water, vacuum dried, and refilled with the desired boric acid solution. An identical volume and reactivity worth determination was then made for each boric acid concentration as had been made for the fuel.

The void reactivity worth correction for the difference in bubble size between fuel- and boric-acid-filled spheres was determined by use of the ZPR-I core center void worth data of appendix C. This correction, as a percent of the total boron-for-fuel substitution reactivity worth, amounted to less than 0.5 percent.

The following sequence of measurements is representative of the procedure used in determining the boron-for-fuel substitution reactivity worth, for a five-ball series, in a ZPR-I base core:

(1) Fuel solution is pumped into the reactor tank until criticality is attained. Critical solution height and solution temperature are recorded. Solution critical height is corrected to 20° C by the temperature coefficient of appendix D.

(2) A fuel-filled plastic ball is held at the core center by the holder of figure 1. Fuel is pumped into the reactor tank until the core is critical. Solution critical height and temperature are recorded. The critical height is corrected to 20° C. (This step is identical for each of the five balls.)

(3) Step 1 is repeated after the experiments indicated in step 2 are completed. The difference between the critical heights of steps 1 and 3 is due to evaporation of water vapor from the fuel solution during the time interval of the series of measurements. The critical height measurements of step 2 are corrected accordingly, if evaporation is assumed to be a linear function of time. The rate of change in solution critical height, due to water evaporation, ranged from about 0.001 centimeter per hour for the 24.892-centimeter base core to approximately 0.005 centimeter per hour for the 67.310-centimeter base core. Accordingly, the correction was small for these experiments.

Critical heights of a critical core with the boric acid solution substituted for fuel solution were determined in an identical manner as outlined previously. The difference between the critical height of a fuel-filled and a boric-acid-filled ball for each ball size and boric acid concentration is converted to reactivity worth by the method outlined in appendix B.

Specific Reactivity and Base Core Flux Integral

Since equation (12) is in a form suitable for evaluation, its components may now be considered. The reactivity worth of a boron-for-fuel substitution for each of the three boric acid concentrations in the 45.720-centimeter base core is plotted as a function of substitution volume in figure 2. For small volume insertions, reactivity is a linear func-

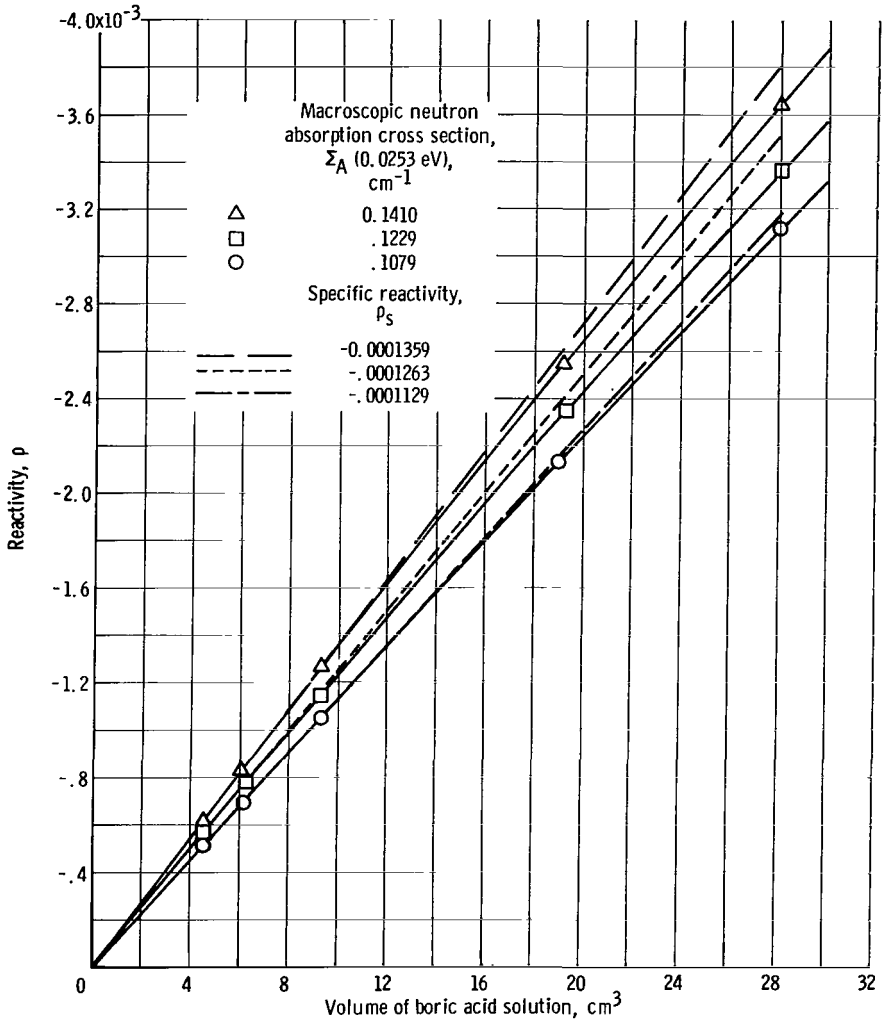

Figure 2. - Reactivity worth of unit spherical volume of boric acid solution of 45.720-centimeter critical ZPR-I core at 20° C. Actual delayed neutron fraction for uranium 235, 0.0064.

tion of substitution volume. The slope of the function, specific reactivity ρ_s (in units of $(\Delta K/K)/cm^3$ based on $\beta = 0.0064$), is drawn for the three boric acid concentrations. The ρ_s thus determined is then plotted as a function of boric acid $\Sigma_A(0.0253\ eV)$ in figure 3. The $\Sigma_A(0.0253\ eV)$ of the fuel solution of this base core is 0.1191 per centimeter. A matching boric acid $\Sigma_A(0.0253\ eV)$ (see fig. 3) corresponds to ρ_s of 0.0001237 per cubic centimeter. Specific reactivities of boron-for-fuel substitutions performed in the other base cores, which were determined in the same manner as stated previously, are given in table V.

In order to evaluate the flux integral of equation (12), the flux $\Phi(\underline{r})$ and adjoint flux $\Phi^*(\underline{r})$ distribution functions must be known. This implies that the extrapolation distance δ to zero neutron flux beyond the core boundaries is also known. Activation of thin

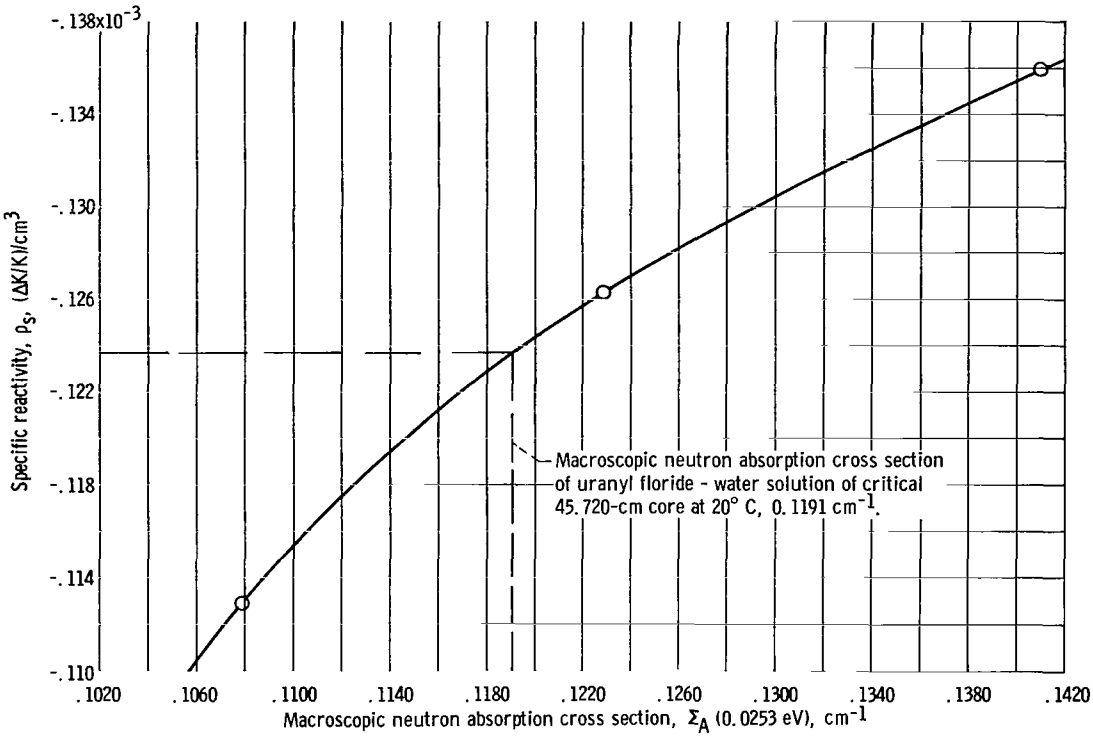

Figure 3. - Specific reactivity of boric acid solutions in center of 45.720-centimeter critical core, as function of boric acid solution macroscopic neutron absorption cross section.

TABLE V. - EXPERIMENTAL RESULTS[a]

Base core critical height at 20° C, cm	Uranyl fluoride - water solution hydrogen to uranium 235 atom ratio, R	Specific reactivity measurements		Absorption cross section mismatch correction, δA	Core flux integral (dysprosium), $\int_V \Phi(\underline{r})\Phi^*(\underline{r})d\underline{r}$, cm^3	Thermal power fraction, f	Core flux integral (total), $\int_V \Phi(\underline{r})\Phi^*(\underline{r})d\underline{r}$, cm^3	Effective delayed neutron fraction, β_{eff} (b)	Effective to actual delayed neutron ratio, γ (b)
		ρ_s, $(\Delta K/K)/cm^3$	ρ_s/β, $/cm^3$ (b)						
24.892	190.1±0.6	-0.0002009	-0.03139±0.00012	0.00139	3221±229	0.910	3540±251	0.0090±0.0006	1.40±0.10
45.720	473.1±3.6	-.0001237	-.01933±0.00008	-.00057	5802±342	.960	6043±357	.0086±0.0005	1.34±0.08
67.310	565.8±4.8	-.00008540	-.01334±0.00005	-.00121	8839±468	.965	9159±485	.0082±0.0004	1.28±0.07

[a]All error limits are 95 percent confidence limits.
[b]$\beta = 0.0064 = 1$ \$.

uranium 235 detectors within a base core provided the correct $\Phi(\underline{r})$ distribution function and core boundary extrapolation distance. The uranium detectors used were 0.635-centimeter-diameter and 0.0279-centimeter-thick uranium-aluminum alloy foils, which contained 15.5 percent uranium by weight. The uranium is 93.3 percent enriched in the uranium 235 isotope. Only one core traverse with uranium 235 detectors was necessary since axial and radial mapping in all of the base core sizes had previously been done with dysprosium detector foils. It will be shown that the flux integral obtained from the dysprosium foil activity distribution can be corrected to the flux integral obtained from the

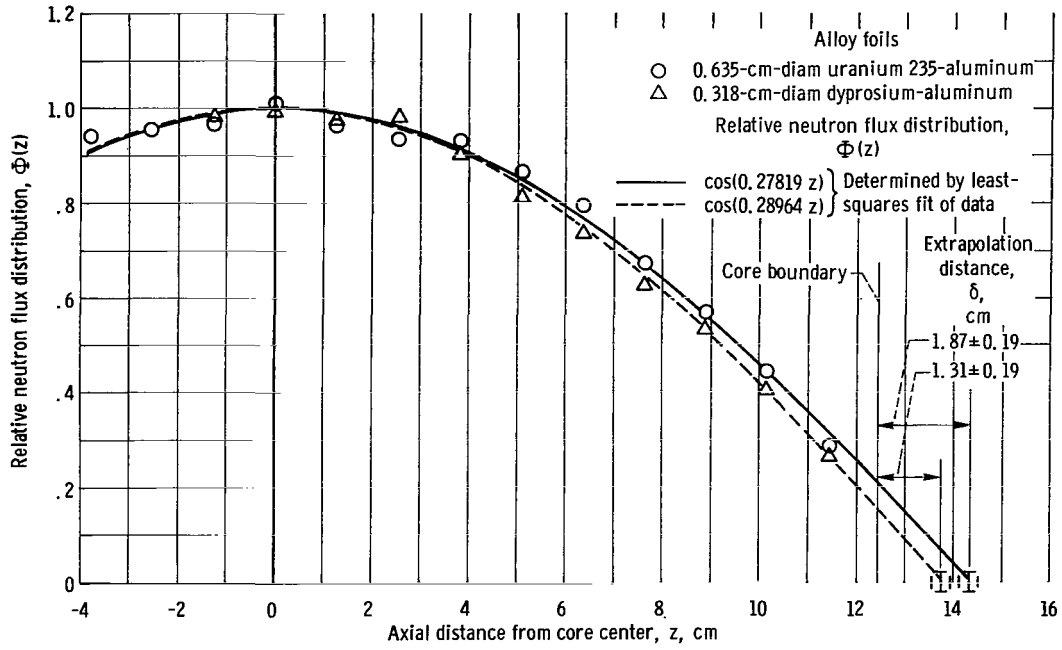

Figure 4. - Determination of extrapolation distance of neutron flux distribution along vertical axis of ZPR-I core using uranium 235 and dysprosium foil activations. Base core height, 24.892 centimeters.

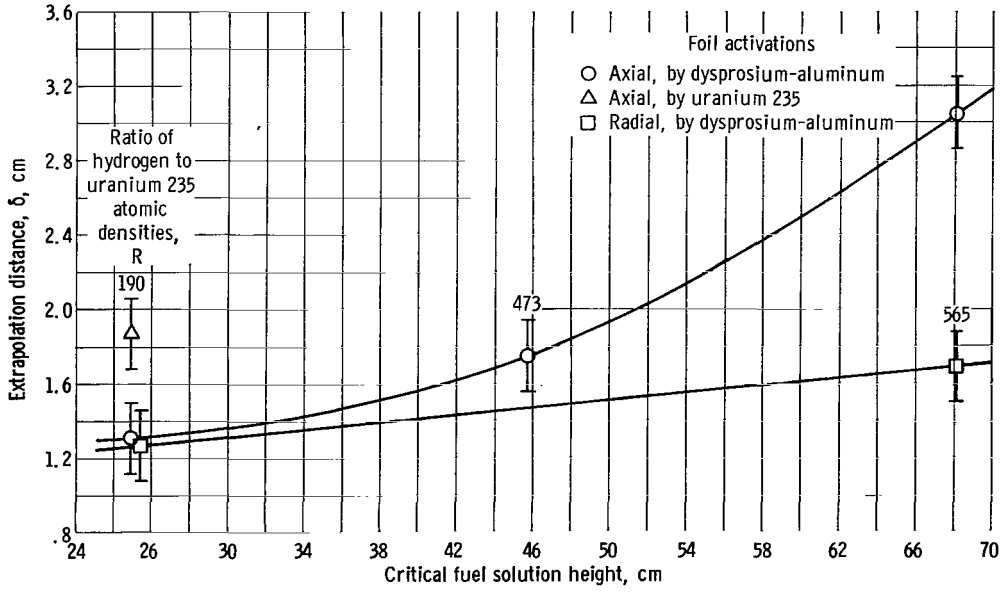

Figure 5. - Extrapolation distance beyond axial and radial core boundaries as function of ZPR-I critical core solution height. Error limits, ±1 standard deviation.

uranium 235 distribution. The dysprosium detectors used were 0.3175-centimeter-diameter and 0.0127-centimeter-thick dysprosium-aluminum alloy foils. The alloy was 5 percent dysprosium by weight.

Foil activation data were fitted in the axial and radial directions by $\cos(\pi z/Z)$ and $J_0[2.405(r/Y)]$ functions, respectively. Both uranium 235 and dysprosium axial distributions for the 24.892-centimeter core are plotted in figure 4. A least-squares fit of the two sets of data by a $\cos(\pi z/Z)$ function resulted in a value of δ of 1.31 centimeters by the dysprosium foil activations and 1.87 centimeters by the uranium 235 foil activations. Similar neutron flux distributions for the other base core sizes were obtained. A plot of the resulting δ as a function of critical core height is shown in figure 5.

If it is assumed that δ is energy independent and $\Phi(\underline{r})$ and $\Phi^*(\underline{r})$ of equation (12) have the same spatial distribution, the product $\Phi(\underline{r})\Phi^*(\underline{r})$ would then be equal to Φ^2, which is the square of the experimentally measured neutron flux distribution. To verify a Φ^2 dependence of reactivity worth variation over the core volume, a boric-acid-filled sphere, having the same $\Sigma_A(0.0253\ \text{eV})$ as the core fuel solution, was traversed both axially and radially in the 24.892-centimeter core. The largest sphere (28.30 cm^3 volume) was used in order to provide measureable reactivities of sufficient magnitude in core regions of least importance. However, the combination of large sphere size and small core volume enhanced the positional errors. The resulting relative reactivity data points, with their estimated positional errors, are plotted in figures 6 and 7. The data appear to follow the Φ^2 distribution reasonably well. The flux integral of equation (12) was evaluated for the base core sizes, utilizing the measured δ and flux distributions discussed previously.

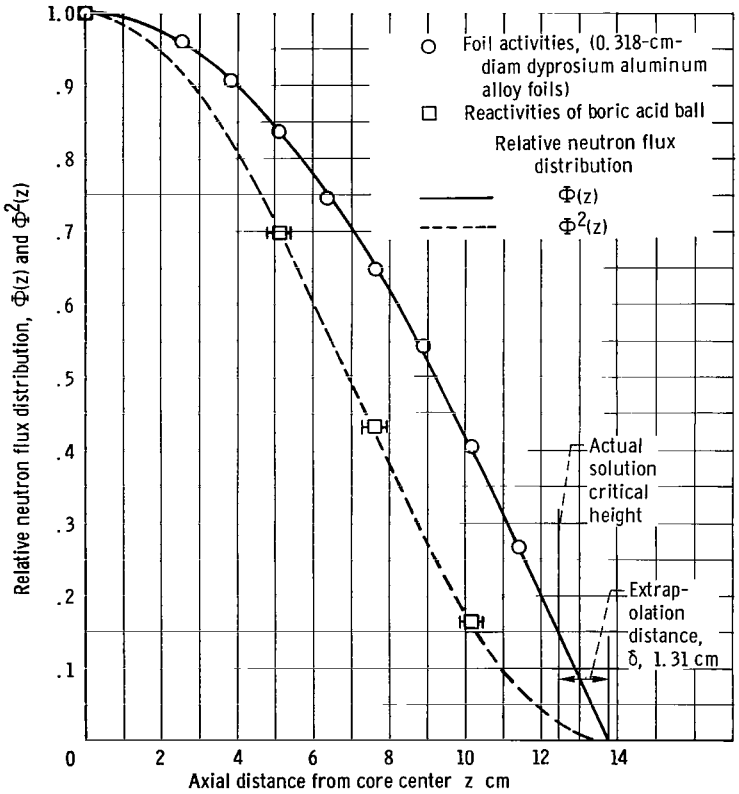

Figure 6. - Relative neutron flux distribution as function of distance along vertical axis from center of a critical cylindrical core. Base core height, 24.892 centimeters.

The flux distributions obtained from dysprosium foil activations were essentially thermal since the cadmium ratios (ref. 17) of the activated dysprosium foils in the base cores were greater than 100. Therefore, the uranium 235 foils

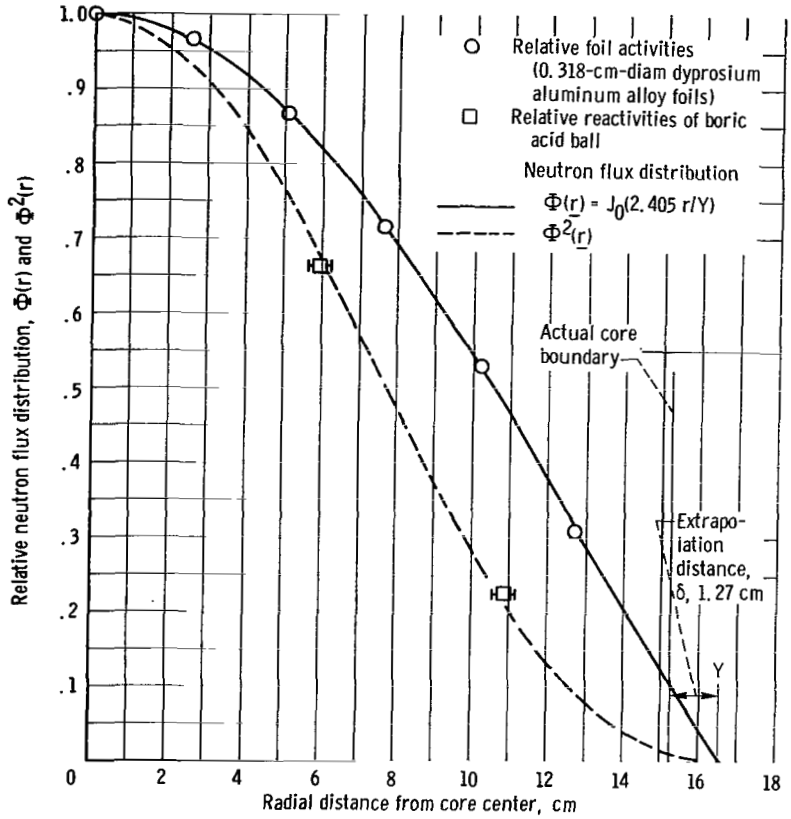

Figure 7. - Relative neutron flux distribution as function of distance along radius from center of critical cylindrical core. Base core height, 24.892 centimeters.

indicated the total fission rate while dysprosium foils indicated only the thermal fission rate. The ratio of the flux integral using the dysprosium extrapolation distance to the flux integral using the uranium 235 extrapolation distance should then be representative of the ratio of the thermal fission rate to the total fission rate f. This was verified to within 3 percent with a diffusion theory calculation assuming a dysprosium "cutoff" of about 3 electron volts. The uranium 235 traverse was performed only for the 24.892-centimeter core and calculated values of f were then used for the other two cores. The values of f and the total flux integral are given in table V (p. 13). These flux integrals have been normalized according to equation (11).

Experimental Determination of Effective Delayed Neutron Fraction

The results presented in table V include the measured specific reactivities of the boron-for-fuel substitutions performed in the three base cores and the corresponding flux integrals. The flux integrals that utilized dysprosium foil activations for relative neutron flux distributions represent the contribution of thermal neutrons only. Division of this

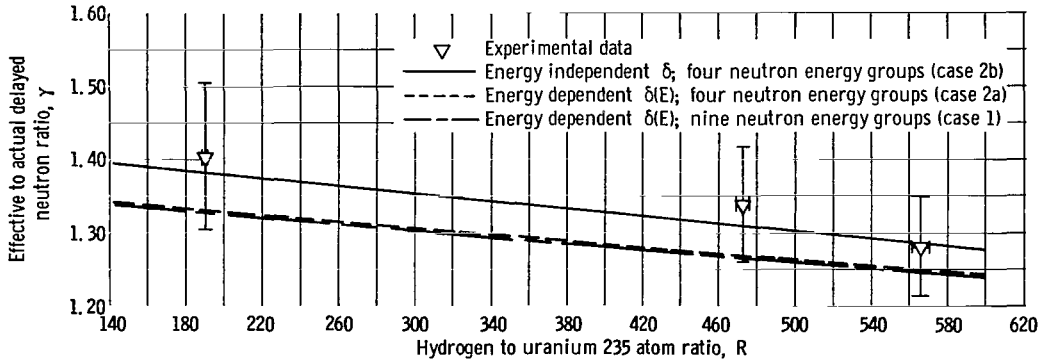

Figure 8. - Effective to actual delayed neutron ratio as function of hydrogen to uranium 235 atom ratio (95 percent confidence limits). Actual delayed neutron fraction for uranium 235, 0.0064.

integral by the thermal power fraction f results in the total core flux integral. This total flux integral weights effectively the specific reactivities by a power distribution that includes neutrons of all energies. The effective delayed neutron fraction β_{eff} is calculated from equation (12) using the specific reactivities and total flux integrals for the base cores of table V. Shown in table V is the experimentally determined ratio $\gamma = \beta_{eff}/\beta$ for the three base cores. Values of γ, as a function of R, are also plotted in figure 8.

The accuracy of the determination of β_{eff} depends on the precision of the specific reactivity ρ_s and the base core flux integral measurements. The standard deviation s of ρ_s is less than ±0.2 percent for all boron-for-fuel substitutions. The standard deviation of the measurement of critical core extrapolation distance δ is ±0.19 centimeter. A 95-percent confidence limit of ±0.38 centimeter (2s) applied to the extrapolation distances results in error limits of ±29, ±22, and ±12 percent for the ZPR-I reactors having 24.892-, 45.720-, and 67.310-centimeter heights, respectively. The corresponding error limits in the base core flux integrals are ±7.1, ±5.9, and ±5.3 percent. The error limits of β_{eff} are, therefore, essentially the same as the error limits of the base core flux integrals. The standard deviations in the determination of the hydrogen to uranium 235 atom ratio R for the three base cores 190.1, 473.1, and 565.8 are ±0.16, ±0.38, and ±0.42 percent, respectively.

THEORETICAL CALCULATIONS FOR EFFECTIVE DELAYED NEUTRON FRACTION

Theoretical calculations for β_{eff} are made for each reactor using the "parallel group" technique described in reference 7. This technique is particularly useful when multigroup spatial computer programs are available. Usually the number of neutron energy groups required is almost double the number normally required for a calculation of the effective multiplication factor. For bare homogeneous reactors some simplification

TABLE VI. - ENERGY GROUP STRUCTURE

Group	Energy	Uranium 235	
		Prompt fission fraction	Delayed fission fraction
1	14.92 to 0.498 MeV	0.868659	0
2	0.498 to 0.183 MeV	.098832	1.0
3	183 to 11.7 keV	.032508	0
4	11 700 to 0.414 eV	0	0
5	0.414 to 0 eV	0	0

is possible with little loss in accuracy.

The criticality calculations are performed using five neutron energy groups. The linear nature of the equations allows the contributions from the delayed neutrons to be written as separate equations and solved simultaneously, in parallel, with the prompt equations. In this particular group structure, given in table VI, no delayed neutrons appear in group 1; hence, nine equations result. Reference 7 reports the use of four prompt groups and four delayed groups with only one energy group transfer. The extension to more groups with a complete down-scattering transfer matrix is straightforward. These equations, which are written in diffusion theory form, are the following:

$$-D_1^p\nabla^2\Phi_1^p + \left(\Sigma_1^p + \Sigma_{1\to2}^p + \Sigma_{1\to3}^p + \Sigma_{1\to4}^p + \Sigma_{1\to5}^p\right)\Phi_1^p = \frac{X_1^p}{K}S \tag{13a}$$

$$-D_2^p\nabla^2\Phi_2^p + \left(\Sigma_2^p + \Sigma_{2\to3}^p + \Sigma_{2\to4}^p + \Sigma_{2\to5}^p\right)\Phi_2^p = \frac{X_2^p}{K}S + \Sigma_{1\to2}^p\Phi_1^p \tag{13b}$$

$$-D_3^p\nabla^2\Phi_3^p + \left(\Sigma_3^p + \Sigma_{3\to4}^p + \Sigma_{3\to5}^p\right)\Phi_3^p = \frac{X_3^p}{K}S + \Sigma_{1\to3}^p\Phi_1^p + \Sigma_{2\to3}^p\Phi_2^p \tag{13c}$$

$$-D_4^p\nabla^2\Phi_4^p + \left(\Sigma_4^p + \Sigma_{4\to5}^p\right)\Phi_4^p = \Sigma_{1\to4}^p\Phi_1^p + \Sigma_{2\to4}^p\Phi_2^p + \Sigma_{3\to4}^p\Phi_3^p \tag{13d}$$

$$-D_5^p\nabla^2\Phi_5^p + \Sigma_5^p\Phi_5^p = \Sigma_{1\to5}^p\Phi_1^p + \Sigma_{2\to5}^p\Phi_2^p + \Sigma_{3\to5}^p\Phi_3^p + \Sigma_{4\to5}^p\Phi_4^p \tag{13e}$$

$$-D_6^d\nabla^2\Phi_6^d + \left(\Sigma_6^d + \Sigma_{6\to7}^d + \Sigma_{6\to8}^d + \Sigma_{6\to9}^d\right)\Phi_6^d = \frac{X_6^d}{K}S \tag{13f}$$

$$-D_7^d\nabla^2\Phi_7^d + \left(\Sigma_7^d + \Sigma_{7\to8}^d + \Sigma_{7\to9}^d\right)\Phi_7^d = \Sigma_{6\to7}^d\Phi_6^d \tag{13g}$$

$$-D_8^d\nabla^2\Phi_8^d + \left(\Sigma_8^d + \Sigma_{8\to9}^d\right)\Phi_8^d = \Sigma_{6\to8}^d\Phi_6^d + \Sigma_{7\to8}^d\Phi_7^d \tag{13h}$$

$$-D_9^d \nabla^2 \Phi_9^d + \Sigma_9^d \Phi_9^d = \Sigma_{6\to9}^d \Phi_6^d + \Sigma_{7\to9}^d \Phi_7^d + \Sigma_{8\to9}^d \Phi_8^d \tag{13i}$$

where

$$S = \sum_{g=1}^{5} \nu\Sigma_{f,g}^p \Phi_g^p + \sum_{g=6}^{9} \nu\Sigma_{f,g}^d \Phi_g^d$$

and

$$\Sigma = \Sigma_a + DB_z^2$$

These nine equations are solved using a one-dimensional diffusion theory program for the IBM 7094 computer system. The macroscopic cross sections for the first four groups are averages over a spectrum resulting from the prompt spectrum of uranium 235 fission neutrons as obtained from a proprietary program GAM-II (ref. 11). The TEMPEST program (ref. 12) is used to obtain the macroscopic cross sections for the thermal groups 5 and 9. A Wigner-Wilkins spectrum is assumed. The cross sections for the delayed groups 6, 7, and 8 are obtained from GAM-II using a fission spectrum of delayed neutrons with a mean energy of 450 keV (refs. 13 and 14).

The first solution of the nine equations is obtained using the following fission fraction values:

$$X_1^p = X_1$$

$$X_2^p = X_2 - \beta$$

$$X_3^p = X_3$$

$$X_6^d = \beta$$

where $\sum_i X_i = 1.0$ and the X_i are given in table VI. The resulting eigenvalue is K_1. Next, the same set of equations is solved with a perturbation to X_6^d; that is, $X_6^d = 2\beta$ and $\sum_i X_i = 1 + \beta$. The eigenvalue is K_2, and β_{eff}/β is given by

$$\frac{\beta_{eff}}{\beta} = \frac{K_2 - K_1}{K_2 K_1 \beta}$$

For bare homogeneous reactors, it is not necessary to use the preceding method. Since the delayed neutrons have the same spatial distribution as the prompt neutrons and the spatial solutions are cosine and Bessel functions, the ratio β_{eff}/β can be obtained by solving only the last four equations with $X_6^d = 1$. The eigenvalue may be interpreted as β_{eff}/β. The critical geometry is assumed such that a solution of the first five equations gives $K = 1$. To be consistent with the previous definition of β_{eff}/β, the following relations are used:

$$\frac{\beta_{eff}}{\beta} = \frac{K_2 - K_1}{K_2 K_1 \beta}$$

for nine group cases, and

$$\frac{\beta_{eff}}{\beta} = \frac{(K_2\beta + K_1) - K_1}{(K_2\beta + K_1)K_1\beta}$$

$$= \frac{K_2}{(K_2\beta + K_1)K_1}$$

for four group cases.

A summary of the calculations is given in table VII. Case 1 is based on the nine

TABLE VII. - CALCULATED RESULTS FOR EFFECTIVE TO ACTUAL DELAYED NEUTRON RATIO

Case	Ratio of hydrogen and uranium 235 atom density, R	Effective multiplication factor of a reactor		Effective to actual delayed neutron ratio, β_{eff}/β	
		First, K_1	Second, K_2	Theoretical	Experimental
1	190	1.000401	1.008999	1.3268	1.40
	473	1.001275	1.009484	1.2650	1.34
	562	1.000821	1.008900	1.2463	1.28
2a	190	1.000169	1.3413	1.3294	1.40
	473	1.001085	1.2809	1.2677	1.34
	562	1.000647	1.2606	1.2489	1.28
2b	190	1.000679	1.3946	1.3804	1.40
	473	1.000473	1.3200	1.3077	1.34
	562	1.000464	1.2976	1.2857	1.28

group solution for each of the three reactors. Case 2 is based on the four delayed groups only. Case 2a, as well as case 1, uses energy-dependent extrapolation distances $\delta(E) = 0.71\ \lambda_{tr}$, while case 2b uses an equivalent energy independent extrapolation distance δ which is equivalent in the sense that δ is chosen so that criticality is computed to approximately the same accuracy as when using $\delta(E)$.

Cases 1 and 2a are in agreement and both are calculated with an energy-dependent extrapolation distance. Case 2b, if energy-independent extrapolation distances are used, gives significantly higher values of β_{eff}/β. It is this case that is most directly comparable with the experiment, since energy independent extrapolation distances are assumed in the experiment also.

Lewis Research Center,
National Aeronautics and Space Administration,
Cleveland, Ohio, June 7, 1966,
122-28-03-02-22.

APPENDIX A

SYMBOLS

B_z^2	transverse buckling, cm^{-2}
C	constant
D	diffusion coefficient, cm
E, E'	energy, eV
f	thermal power fraction ratio of thermal fission rate to total fission rate
f(E), f(E')	fraction of fission neutrons per unit energy
H	modified critical height of core, h plus 9.8 cm, cm
ΔH	incremental change in critical core height, cm
h	actual critical height of a ZPR-I core, cm
i	i^{th} substitution
J_0	Bessel function of first kind of zero order
j	j^{th} group
K	effective multiplication factor of a reactor
K_1, K_2	eigenvalues
$\Delta K/K$	(K - 1)/K
ℓ	mean prompt neutron lifetime, sec
N	atom density, $atom/cm^3$
$P(\underline{r})$	neutron production rate at position $\underline{r}$ per cm^3, $\sum_g \nu(\Sigma_f)_g(\underline{r})\Phi_g(\underline{r})$ for g energy groups of neutrons
$P^*(\underline{r})$	fission spectrum weighted adjoint at position $\underline{r}$ per cm^3, $\sum_g X_g \Phi_g^*(\underline{r})$ for g energy groups of neutrons
R	ratio of hydrogen to uranium 235 atom densities
r	distance along a radius perpendicular to axial core centerline, cm
$\underline{r}$	position vector
S	fission source including both prompt and delayed neutrons

s	standard deviation
T	stable reactor period, sec
T_i	stable reactor period corresponding to i^{th} substitution, sec
Δt	incremental change in fuel solution temperature
V	total core volume
X	neutron fission fraction for given energy group
Y	actual critical core radius plus δ
Z	actual critical height plus 2δ
z	distance from core center to point on cylinder axis, cm
β	actual delayed neutron fraction for uranium 235, $\sum_{j=1}^{6} \beta_j$
β_{eff}	effective delayed neutron fraction (see eq. (12))
β_j	fraction of total fission neutrons in j^{th} delayed group
γ	effective to actual delayed neutron ratio, β_{eff}/β
δ	energy independent extrapolation distance from reactor core boundary to point at which flux is zero
δA	absorption cross section reactivity mismatch correction (see eq. (7))
$\delta(E)$	energy dependent extrapolation distance, cm
$\delta\rho_{\tau_i}$	incremental reactivity worth of substitution of nonfissionable material for fissionable material in core region τ_i of critical reactor
$\delta\Sigma_a$	incremental perturbation in Σ_a
λ_j	decay constant for j^{th} group of delayed neutrons, sec^{-1}
λ_{tr}	transport mean free path, cm
$\nu\Sigma_f$	number of neutrons per fission times fission cross section, neutrons/cm
ρ	reactivity, $\Delta K/K$ based on $\beta = 0.0064$
$\Delta\rho$	incremental change in reactivity associated with incremental change in critical core height, ΔH
ρ_s	specific reactivity, reactivity per cm^3 of boron-for-fuel substitute

$\Sigma_A(0.0253\ \text{eV})$	macroscopic neutron absorption cross section at 0.0253 eV, cm^{-1}
Σ_a	macroscopic absorption cross section for a given energy group, cm^{-1}
$\Sigma_{g \to g+n}$	transfer cross section from energy group g to group g + n (n = 1, 2, . . . and g + n ≤ total number of energy groups), cm^{-1}
$\sigma_A(0.0253\ \text{eV})$	microscopic neutron absorption cross section at 0.0253 eV, b
τ_i	volume region of i^{th} substitution
Φ^2	square of experimentally measured neutron flux distribution
$\Phi(\underline{r})$	neutron flux at position $\underline{r}$
$\Phi^*(\underline{r})$	adjoint neutron flux at position $\underline{r}$
$\Phi(\underline{r}, E)$	neutron flux per unit energy at $\underline{r}$ and E
$\Phi^*(\underline{r}, E)$ and $\Phi^*(\underline{r}, E')$	adjoint per unit energy at $\underline{r}$ and E or E'
Subscripts:	
calc	calculated values
exp	experimentally determined values
g	energy group numbers, 1, 2, . . ., 9
Superscripts:	
d	delayed neutrons
p	prompt neutrons

APPENDIX B

CALIBRATION OF AN NASA ZPR-I CRITICAL CORE

Introduction

The ZPR-I calibration curve to be derived for an unperturbed core gives directly the reactivity worth of an increment of fuel solution height due to a uniform change of the uranyl fluoride - water fuel solution $\Sigma_A(0.0253\ \text{eV})$. This same calibration curve can be used to determine the reactivity worth of an incremental change in fuel height due to a small core-centered perturbation, up to a certain sample size and reactivity worth. Sample sizes up to nearly 4 centimeters in diameter that have a reactivity worth of nearly a dollar can still be related to reactivity by the unperturbed core calibration curve. The usefulness of these findings are twofold. First, absolute reactivity worths of moderate core centered perturbations (reactivity worth less than 1 \$) can be found easily in a ZPR-I core. Second, the reactivity worth of a perturbation in a certain base core configuration can be found although the measurement may have been performed in a critical core of a slightly different height.

Slope of Unreflected Unperturbed Critical Uranyl Fluoride - Water Solution Core

Reactivity ρ can be calculated from a measured stable reactor period T by the inhour equation (ref. 15)

$$\rho = \frac{\ell}{T} + \gamma \sum_{j=1}^{6} \frac{\beta_j}{1 + \lambda_j T} \tag{B1}$$

The stable reactor period associated with an incremental increase of fuel solution above a critical core height has been measured for several fuel concentrations in ZPR-I. Small increments of fuel were added to a critical reactor to obtain stable reactor periods that were always greater than 200 seconds. For the ZPR-I reactors considered, ℓ varied from about 25 to 60 microseconds. As a result, the reactivities determined can be considered independent of mean prompt neutron lifetime ℓ. Moore's reactivity table (ref. 16), derived from the inhour equation with $\beta = 0.0064$ and $\gamma = 1.0$, was used for convenience in determining reactivities from the measured stable periods. An example of such a determination is shown in figure 9. The slope of this curve is $\Delta\rho/\Delta H$.

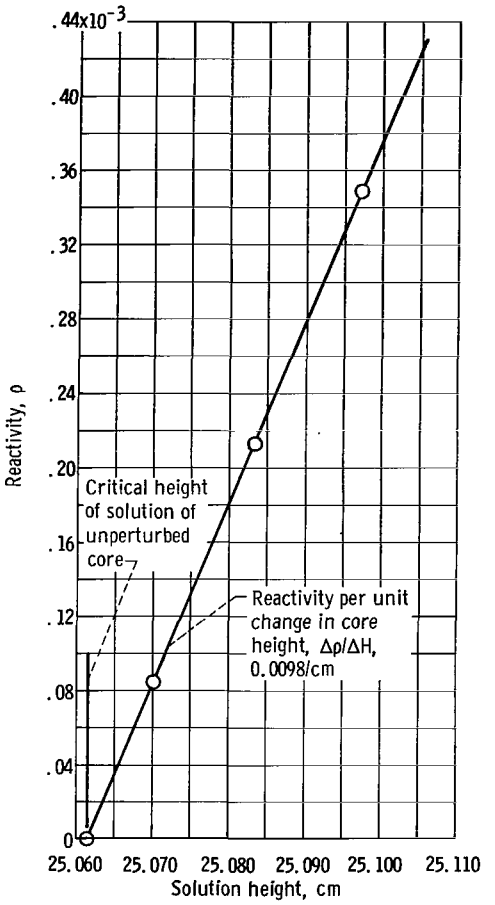

Figure 9. - Reactivity as function of uranyl floride - water fuel solution height above unperturbed critical core. Actual delayed neutron fraction for uranium 235, 0.0064.

When the uranyl fluoride - water solution critical heights are plotted as a function of $(\Delta\rho/\Delta H)^{-1/3}$ on linear graph paper, the data can be fitted by a straight line that intercepts the ordinate a few centimeters below zero critical height. Gwin (ref. 5) presents $\Delta\rho/\Delta H$ data in this manner for several different configurations of the uranyl fluoride - water critical solution geometries. His data extrapolated to an ordinate intercept of -7.5 centimeters. A fit of ZPR-I $\Delta\rho/\Delta H$ data, including Gwin's data from reference 5 for a 30.5-centimeter-diameter critical uranyl fluoride - water core, resulted in an ordinate intercept at -9.8 centimeters as shown in figure 10. If h equals the actual ZPR-I core critical height, then let

$$H = h + 9.8 \text{ cm} \tag{B2}$$

so that

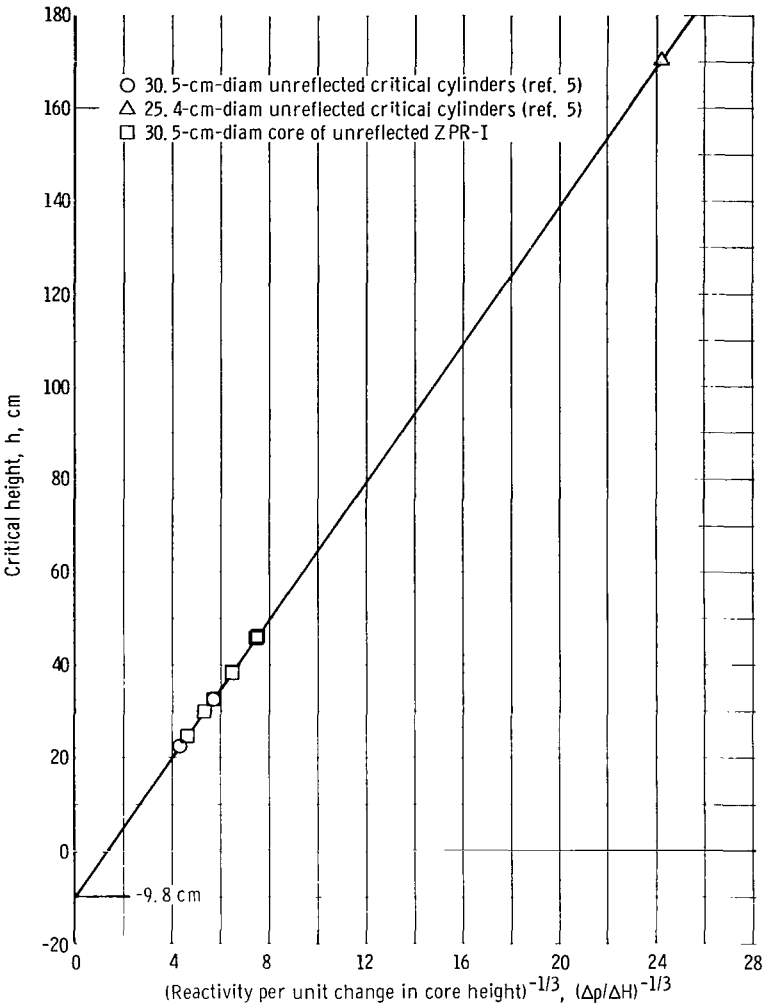

Figure 10. - Critical height as function of (reactivity per unit change in core height)$^{-1/3}$, $(\Delta\rho/\Delta H)^{-1/3}$. Actual delayed neutron fraction for uranium 235, 0.0064.

$$H = C\left(\frac{\Delta\rho}{\Delta H}\right)^{-1/3} \tag{B3}$$

The constant C in equation (B3) is evaluated from figure 10 and equals 7.4303. Equation (B3) can be written as

$$\frac{\Delta\rho}{\Delta H} = 410.22\ H^{-3} \tag{B4}$$

In the limit as $\Delta\rho$ and ΔH approach zero, equation (B4) can be written as the differential $d\rho$, where

$$d\rho = 410.22\ H^{-3}\ dH \qquad \text{(B5)}$$

which can be integrated to obtain reactivity.

Slope of Unreflected Perturbed Critical ZPR-I Cores

A ZPR-I reactor of one critical height can easily be changed to a core of a different critical height by simply adding water to or evaporating water from the uranyl fluoride - water solution. This action changes the hydrogen to uranium 235 atom ratio R and $\Sigma_A(0.0253\ eV)$ of the fuel solution. The $\Delta\rho/\Delta H$ slope of any particular core height can be found from figure 10. If the fuel solution were altered slightly by the uniform addition

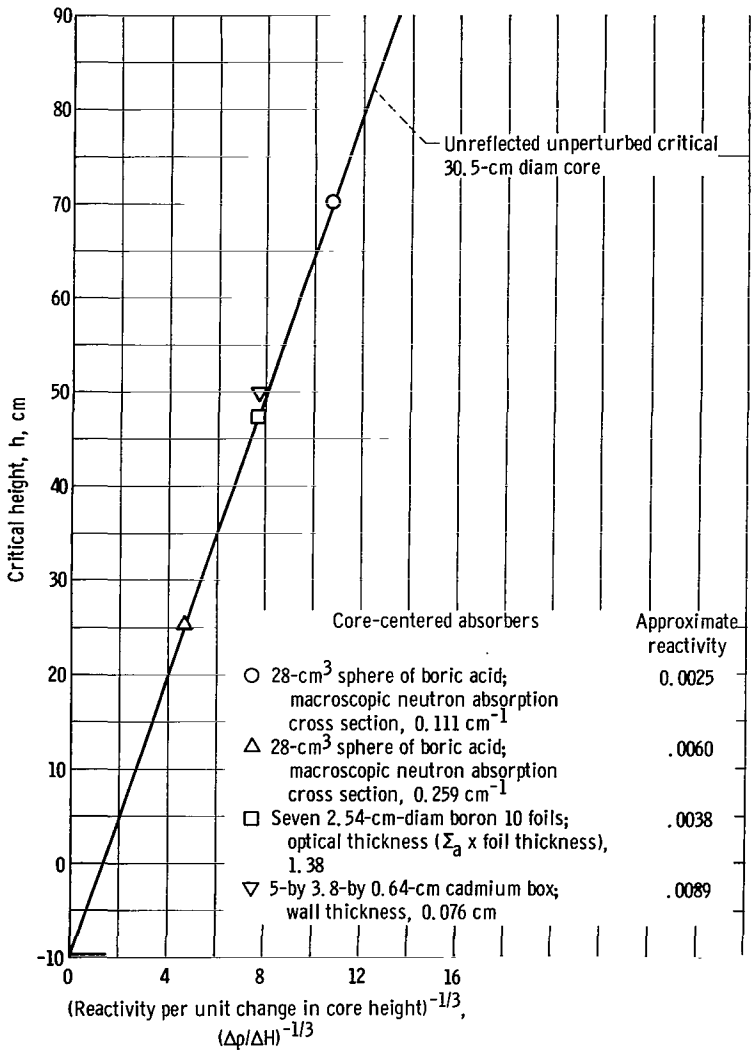

Figure 11. - Critical height as function of (reactivity per unit change in core height)$^{-1/3}$, $(\Delta\rho/\Delta H)^{-1/3}$, for unreflected, perturbed, cylindrical reactors of uranyl fluoride-water solution in aluminum containers. Actual delayed neutron fraction for uranium 235, 0.0064.

of a neutron absorber, for example, boric acid to the fuel solution, and the $\Delta\rho/\Delta H$ slope of this perturbed reactor measured, then this slope is expected to be identical to that of unperturbed core of the same critical height but of a different R ratio.

A comparison of a localized absorber with a uniform dispersion of absorber is desired. A $\Delta\rho/\Delta H$ slope was measured for several ZPR-I critical cores with core-centered perturbations. The results are shown in figure 11, which is basically a reproduction of figure 10 but with the data points of core-centered perturbations superimposed on the unperturbed critical core curve. With the exception of the large cadmium box absorber, the core-centered absorbers shown have $\Delta\rho/\Delta H$ slopes nearly identical to unperturbed critical cores of the same height but a different uranyl fluoride - water solution concentration. The two 28-cubic-centimeter spheres of boric acid solution, of the same $\Sigma_A(0.0253\ \text{eV})$ as the uranyl fluoride - water solutions they were inserted into, represent perturbations at the core center with reactivity worths as high as 0.006 $\Delta K/K$. The seven 2.54-centimeter-diameter foils of boron 10 ($\Sigma_A(0.0253\ \text{eV}) = 1.38$) provided a rather severe core-centered thermal neutron flux perturbation with a reactivity worth of approximately 0.0038 $\Delta K/K$, yet the measured $\Delta\rho/\Delta H$ slope was identical to that of an unperturbed core of the same height. The size of the cadmium box (5- by 3.8- by 0.64-cm) and reactivity worth (about 0.0089 $\Delta K/K$) apparently distorted the thermal neutron flux too severely to be classified as a simple core perturbation.

The specific reactivity ρ_s of the boron-for-fuel core-centered substitution performed for this report depended strongly on the reactivity worth measurement of the smallest ball used (approximately 4.6 cm^3) for determination of unit volume reactivity worth. The measured reactivity worth of this boric-acid-filled ball was much less than 0.001 $\Delta K/K$ for all ZPR-I base core sizes. Based on the data presented in figure 11, it can be seen that use of the H against $(\Delta\rho/\Delta H)^{-1/3}$ functional relation to obtain reactivities is valid for perturbations with reactivities up to approximately one dollar.

Integral Calibration Curve Relating Incremental Change in Core Height to Reactivity

The foregoing discussion and data of figure 11 have shown that the reactivity associated with an incremental change in ZPR-I critical core height ΔH caused by a uniform change in the uranyl fluoride - water solution concentration, is equivalent to a ΔH caused by a moderate core centered perturbation. Therefore, a series of core perturbations made in cores that differ slightly in critical height from day to day, because of the continuous evaporation of water from the fuel solution, can be normalized to a particular base core critical height. An integral calibration curve to normalize the unperturbed critical core heights, and to determine the reactivity worth of a core perturbation, can be obtained by integration of equation (B5):

$$\rho = \int d\rho = 410.22 \int H^{-3}\, dH + C \tag{B6}$$

As an example, consider the 45.720-centimeter-base critical core. Integration of equation (B6) gives

$$\rho = -(205.11)H^{-2} + C \tag{B7}$$

The constant C is evaluated by setting $\rho = 0$ at $H = 45.720 + 9.8 = 55.520$ centimeters so that

$$C = \frac{205.11}{(55.520)^2} = 0.066541 \tag{B8}$$

and the equation for ρ as a function of H is

$$\rho = -(205.11)H^{-2} + 0.066541 \tag{B9}$$

As an example of the use of equation (B9) for the 45.720-centimeter-base core (H = 55.520 cm), one reactivity determination of a boron-for-fuel substitution will be given. The unperturbed core critical height at 20° C is 45.8384 centimeters (H = 55.6384 cm). The reactivity worth of the increment of fuel solution above the base core height is 0.000282 $\Delta K/K$. Next, the critical height at 20° C with a core centered 4.5296-cubic-centimeter ball of boric acid solution ($\Sigma_A(0.0253\ eV) = 0.1229\ cm^{-1}$) is 46.3098 centimeters (H = 56.1098 cm). The reactivity worth of fuel solution and core perturbation is equal to 0.001392 $\Delta K/K$. Thus, the net reactivity worth of the substitution equals 0.001392 - 0.000282 = 0.001110.

Reactivities associated with core centered perturbations in the 24.892- and 67.310-centimeter base critical cores were found in the same manner as for the 45.720-centimeter core. The equations for these two cores are

$$\rho = -(205.11)H^{-2} + 0.170424 \tag{B10}$$

for the 24.892-centimeter core and

$$\rho = -(205.11)H^{-2} + 0.034496 \tag{B11}$$

for the 67.310-centimeter core.

APPENDIX C

REACTIVITY WORTH OF ZPR-I CORE CENTERED VOID

As described in the EXPERIMENTAL PROCEDURE section, a small air bubble remained in each of the boric-acid- and fuel-filled plastic spheres of table II (p. 8). Therefore, it was necessary to measure the reactivity worth of a core-centered void volume in order to obtain a correction for this difference in bubble size. This measurement was accomplished by determining the core-centered reactivity worth of each of the empty plastic spheres. An example of one base core measurement of this void worth is shown in figure 12 for the 45.720-centimeter core. The reactivity per unit volume for small volumes is a linear function of volume with a slope of 5.21×10^{-5}. Figure 13 shows the central core void volume worth of all three base cores.

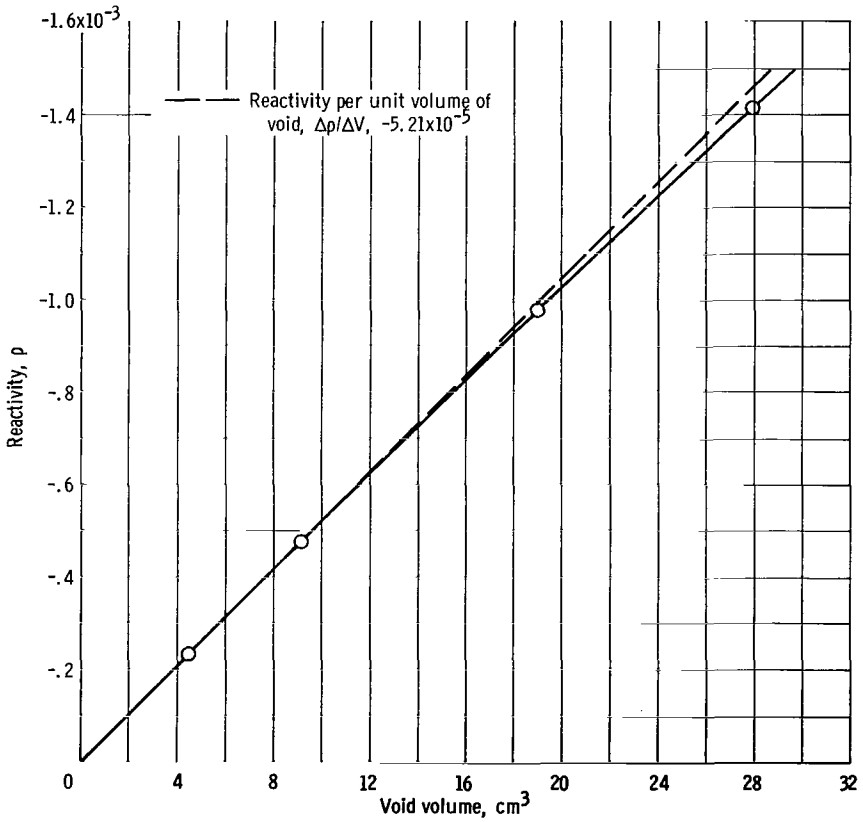

Figure 12. - Worth of void in center of 45.720-centimeter (18.000 in.) critical ZPR-I core at 20° C. Actual delayed neutron fraction for uranium 235, 0.0064.

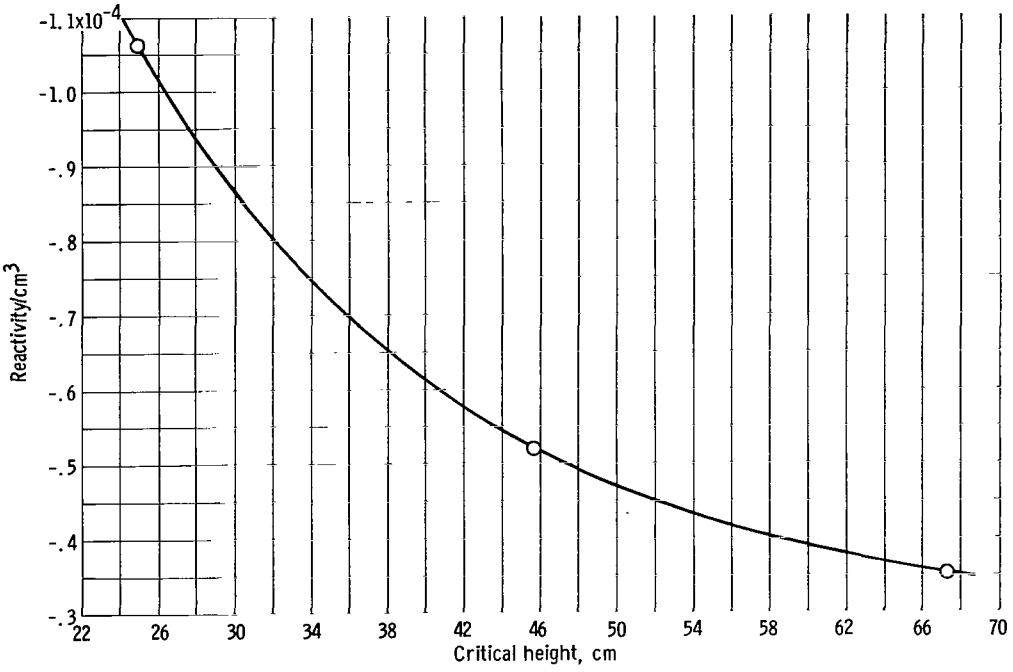

Figure 13. - Core-centered unit volume void worth as function of ZPR-I critical core height at 20° C. Actual delayed neutron fraction for uranium 235, 0.0064.

APPENDIX D

TEMPERATURE COEFFICIENT OF REACTIVITY FOR AN NASA ZPR-I REACTOR

The ZPR-I is operated at very low power and therefore undergoes no temperature change as a result of heat generation within the core. The variation of fuel temperature is caused by the change in the reactor room air temperature. The reactor room is provided with a heating system and an exhaust fan for ventilation but not with any air conditioning equipment. Day to day changes in room air temperature are usually slight. Longer term seasonal temperature variation causes gradual room air temperature change from approximately 20° to 25° C.

For a reactor temperature coefficient determination, the critical height of the ZPR-I fuel solution at normal room temperature is first measured. The reactor room air is then heated until approximately a 2° to 5° C increase in fuel solution temperature occurs. The new critical height of the warmer fuel solution is then measured. The ratio of the incremental difference between these two critical heights ΔH to the number of degrees change in solution temperature Δt that had occurred is the temperature coefficient. This coefficient has been found to be a constant over the temperature range involved within the accuracy of the measurement.

The temperature coefficient $\Delta H/\Delta t$ was measured for three base cores having critical heights of 24.892, 45.720, and 67.310 centimeters. These temperature coefficients as functions of ZPR-I critical fuel solution height are plotted in figure 14. Temperature coefficients in reactivity per degree centigrade $\Delta\rho/\Delta t$ for the same base cores were obtained by converting the ΔH of figure 14 to $\Delta\rho$ from figure 10 (p. 27). The resulting reactivity temperature coefficient as a function of critical height is plotted in figure 15.

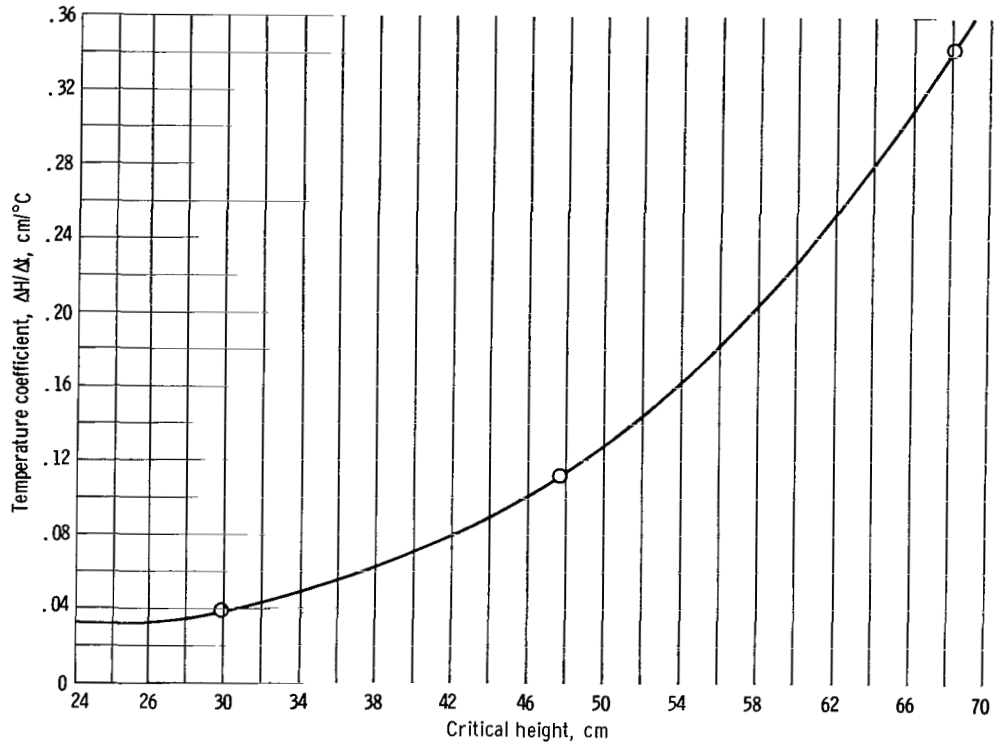

Figure 14. - Temperature coefficient as function of ZPR-I critical height. Temperature range, 20° to 26° C.

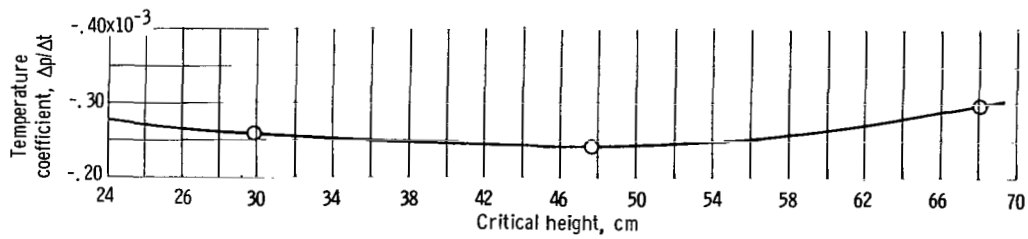

Figure 15. - Temperature coefficient obtained from figures 10 and 14. Actual delayed neutron fraction for uranium 235, 0.0064; temperature range, 20° to 26° C.

REFERENCES

1. Anderson, H. L.; Fermi, E.; Wattenberg, A.; Weil, G. L.; and Zinn, W. H.: Method for Measuring Neutron-Absorption Cross Sections by the Effect on the Reactivity of a Chain-Reacting Pile. Phys. Rev., vol. 72, no. 1, July 1947, pp. 16-21.

2. Weinberg, Alvin M.; and Wigner, Eugene P.: The Physical Theory of Neutron Chain Reactors. Univ. of Chicago Press, 1958.

3. Gross, E. E.; and Marable, J. H.: Static and Dynamic Multiplication Factors and Their Relation to the Inhour Equation. Nucl. Sci. Eng., vol. 7, no. 4, Apr. 1960, pp. 281-291.

4. Henry, A. F.: The Application of Reactor Kinetics to the Analysis of Experiments. Nucl. Sci. Eng., vol. 3, no. 1, 1958, pp. 52-70.

5. Gwin, R.; Trubey, D. K.; and Weinberg, A. M.: Experimental and Theoretical Studies of Unreflected Aqueous U-235 Critical Assemblies. Vol. 12 of Proc. of the Second United Nations Conf. on Peaceful Uses of Atomic Energy, United Nations, 1958, pp. 529-538.

6. Ruane, T. F.; Anthony, D. J.; Buck, P.; Gavin, D. A.; and Stewart, H. B.: A Measurement of the Effective Delayed Neutron Fraction by the Substitution Method. ANS Trans., vol. 1, no. 2, Dec. 1958, pp. 142-144.

7. Kaplan, S.; and Henry, A. F.: An Experiment to Measure Effective Delayed Neutron Fractions. Rep. No. WAPD-TM-209, Westinghouse Electric Corp., Feb. 1960.

8. Perez-Belles, R.; Kington, J. D.; and De Saussure, G.: A Measurement of the Effective Delayed Neutron Fraction for the Bulk Shielding Reactor-I. Nucl. Sci. Eng., vol. 12, no. 4, Apr. 1962, pp. 505-512.

9. Henry, A. F.: Computation of Parameters Appearing in the Reactor Kinetics Equations. Rep. No. WAPD-142, Westinghouse Electric Corp., Dec. 1955.

10. Fox, Thomas A.; Mueller, Robert A.; Ford, C. Hubbard; and Alger, Donald L.: Critical Mass Studies with NASA Zero Power Reactor II. I - Clean Homogeneous Configurations. NASA TN D-3097, 1965.

11. Joanou, G. D.; and Dudek, J. S.: GAM-II. A B_3 Code for the Calculation of Fast-Neutron Spectra and Associated Multigroup Constants. Rep. No. GA-4265, General Atomics, July 1963.

12. Shudde, R. H.; and Dyer, J.: Tempest. A Neutron Thermalization Code. Atomics International, Sept. 1960.

13. Anon.: Reactor Physics Constants. Rep. No. ANL-5800 (2nd ed.), Argonne National Lab., July 1963, p. 618.

14. Keepin, G. R.; Wimett, T. F.; and Zeigler, R. K.: Delayed Neutrons from Fissionable Isotopes of Uranium, Plutonium, and Thorium. Phys. Rev., vol. 107, no. 4, Aug. 1957, pp. 1044-1049.

15. Glasstone, Samuel; and Edlund, Milton C.: The Elements of Nuclear Reactor Theory. D. Van Nostrand Co., Inc., 1952, p. 301.

16. Moore, K. V.: Tables of Reactivity vs. Period for U^{235}, Pu^{239}, and U^{233}. Rep. No. IDO-16485, Phillips Petroleum Co., Sept. 10, 1958.

17. Hughes, Donald J.: Pile Neutron Research. Addison-Wesley Publ. Co., Inc., 1953, p. 62.

"The aeronautical and space activities of the United States shall be conducted so as to contribute . . . to the expansion of human knowledge of phenomena in the atmosphere and space. The Administration shall provide for the widest practicable and appropriate dissemination of information concerning its activities and the results thereof."

—NATIONAL AERONAUTICS AND SPACE ACT OF 1958

NASA SCIENTIFIC AND TECHNICAL PUBLICATIONS

TECHNICAL REPORTS: Scientific and technical information considered important, complete, and a lasting contribution to existing knowledge.

TECHNICAL NOTES: Information less broad in scope but nevertheless of importance as a contribution to existing knowledge.

TECHNICAL MEMORANDUMS: Information receiving limited distribution because of preliminary data, security classification, or other reasons.

CONTRACTOR REPORTS: Technical information generated in connection with a NASA contract or grant and released under NASA auspices.

TECHNICAL TRANSLATIONS: Information published in a foreign language considered to merit NASA distribution in English.

TECHNICAL REPRINTS: Information derived from NASA activities and initially published in the form of journal articles.

SPECIAL PUBLICATIONS: Information derived from or of value to NASA activities but not necessarily reporting the results of individual NASA-programmed scientific efforts. Publications include conference proceedings, monographs, data compilations, handbooks, sourcebooks, and special bibliographies.

Details on the availability of these publications may be obtained from:

SCIENTIFIC AND TECHNICAL INFORMATION DIVISION

NATIONAL AERONAUTICS AND SPACE ADMINISTRATION

Washington, D.C. 20546